Crack-microcrack interactions in dynamical fracture

Eran Bouchbinder,[1] David Kessler,[2] and Itamar Procaccia[1]
[1]*Department of Chemical Physics, The Weizmann Institute of Science, Rehovot 76100, Israel*
[2]*Department of Physics, Bar-Ilan University, Ramat Gan 52900, Israel*
(Received 28 March 2004; published 19 October 2004)

We address the interaction of fast moving cracks in stressed materials with microcracks on their way, considering it as one possible mechanism for fluctuations in the velocity of the main crack (irrespective whether the microcracks are existing material defects or they form during the crack evolution). We analyze carefully the dynamics (in two space dimensions) of one macrocrack and one microcrack, and demonstrate that their interaction results in a *large* and *rapid* velocity fluctuation, in qualitative correspondence with typical velocity fluctuations observed in experiments. In developing the theory of the dynamical interaction we invoke an approximation that affords a reduction in mathematical complexity to a simple set of ordinary differential equations for the positions of the crack tips; we propose that this kind of approximation has a range of usefulness that exceeds the present context.

DOI: 10.1103/PhysRevE.70.046107 PACS number(s): 62.20.Mk, 46.50.+a

I. INTRODUCTION

Classical linear elasticity fracture mechanics provides clear cut predictions for the dynamical evolution of cracks in stressed materials. Consider a crack in an infinite medium under a tensile load at infinity. Such a crack is expected to remain straight, and to exhibit a tip velocity that increases monotonically towards the Rayleigh wave speed c_R. Reality shows that this is but a pipe dream. When the crack velocity exceeds a finite fraction of c_R the velocity of typical cracks exhibits wild fluctuations, the crack surfaces lose their smoothness and the mean velocity never asymptotes towards c_R. The fundamental understanding of the discrepancy between the prediction of the classical theory and experiments remains an open problem of considerable interest and importance.

A number of studies [1–8] point towards a close correspondence between the onset of velocity fluctuations and the appearance of secondary damage like microcracks (appearing ahead of the tip), microscopic side branches, etc. Conical markings which are observed on crack surfaces offer a good indication that microcracks exist before the arrival of the crack, although it is not determined whether the former stem from material imperfections or from stress instabilities. The fact that the density of conical markings increases during the crack evolution [5] suggests that the level of stress is responsible in some way for the activation of the microcracks. The aim of this paper is to explore the connection between velocity fluctuations and the putative existence of microcracks ahead of the crack tip. To this aim we study the dynamical interaction between a macrocrack and a microcrack and focus on the velocity of the tip of the former under the influence of the latter.

To actually solve exactly the dynamical equations for the displacement field with boundary condition on both macrocrack and microcrack up to coalescence is a very taxing quest. Building upon experience in the field we will propose here an approximate methodology that will allow us to write down *ordinary* differential equations for the positions of the tips of both macrocrack and microcrack. While sensible, the approximate methodology is not established in a controlled fashion, requiring therefore simulational support. Indeed, we will offer in this paper lattice simulations to back the analytic considerations. We will show that the correspondence is excellent.

In Sec. II we introduce the problem at hand, being an infinite two-dimensional stressed material with one macrocrack and one collinear microcrack of length ℓ. In Sec. III we describe the approximate method of solution, motivating it by the exactly soluble cases of straight and bifurcating cracks. The section culminates with approximate equations of motion for the tips of the macrocrack and microcrack. In Sec. IV we describe the solution of the model problem, stressing the velocity of the tip of the macrocrack. We show that the net result of the interaction is a rapid and large up and down fluctuation in this velocity, in correspondence with the observed fluctuations in dynamical crack propagation. Section V provides a simulational support to the approximate theory; by performing lattice simulations we study the same model problem and compare the results. The close correspondence between approximate theory and simulations lends support to the former. Section VI offers a summary and conclusions.

II. THE PROBLEM

The problem that we want to consider is sketched in Fig. 1. We consider a macrocrack and a microcrack that at a given time extend along the intervals $[-L,0]$ and $[\ell_-,\ell_+]$, respectively. The distance between them is given by Δ. The length

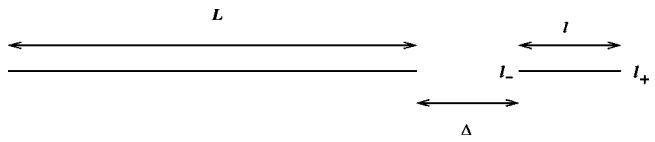

FIG. 1. The geometric configuration of the model problem. The macrocrack and the microcrack extend along the intervals $[-L,0]$ and $[\ell_-,\ell_+]$, respectively, with $L/\ell \gg 1$.

 ©2004 The American Physical Society

of the microcrack is $\ell \equiv \ell_+ - \ell_-$. We expect on physical grounds that the microcracks in typical materials are at most of the size of the process zone, and therefore we always consider the limit $\ell/L \to 0$.

The aim of the calculation is to determine the simultaneous motion of the three crack tips (the macrocrack tip, the inner and outer tips of the microcrack) as a function of time. In full generality this entails the general solution of the field equations for an arbitrary motion, specifically the determination of the *dynamic* stress intensity factors at the crack tips and then to apply a fracture criterion to obtain the actual dynamics. We cannot offer an exact solution to this problem. Instead, we will introduce an approximate method that provides analytic insight to the problem.

III. APPROXIMATE METHOD OF SOLUTION

To motivate our approximate methodology we will recall some exact classical results obtained for ideal (mode I) straight dynamical cracks and more recent results pertaining to (mode III) bifurcating cracks.

A. Motivation I: Ideal straight cracks

As said above, linear elasticity fracture mechanics provides exact solutions for straight cracks under mode I loading. The stress field $\sigma_{ij}(r,\theta,t)$, measured in polar coordinates relative to the tip, is expected to have a universal form in the vicinity of the crack tip [9],

$$\sigma_{ij}(r,\theta,t) = K_{\rm I}(v(t),L(t))\frac{\Sigma^{\rm I}_{ij}(\theta,v(t))}{\sqrt{2\pi r}}. \tag{1}$$

Here $v(t)$ and $L(t)$ are the time-dependent crack velocity and length, respectively, $\Sigma^{\rm I}_{ij}(\theta,v)$ are known universal functions [9], and $K_{\rm I}(v,L)$ is the "stress intensity factor" which is predicted to depend on the instantaneous crack velocity and length *only*. For notational simplicity we drop the t dependence. At each moment in time the velocity is expected (for plane stress conditions) to be determined by the energy balance equation [9]

$$\Gamma(v) = \frac{1}{E}A_{\rm I}(v)K^2_{\rm I}(v,L). \tag{2}$$

The left-hand side (LHS) here is the fracture energy and the right-hand side (RHS) is the energy release rate into the crack tip region, resulting from a path integral over the energy flux. E is Young's modulus and $A_{\rm I}(v)$ is a mode I universal function. The exact result that we refer to is the decomposition of the dynamic stress intensity factor $K_{\rm I}(v,L)$ for a semi-infinite crack under time independent loading, in the form [9–11]

$$K_{\rm I}(v,L) = k_{\rm I}(v)K^s_{\rm I}(L), \tag{3}$$

where $k_{\rm I}(v)$ is a universal function of v and $K^s_{\rm I}(L)$ is the stress intensity factor of a *static* crack of length L under the same loading (when L is large enough to be considered as semi-infinite). This important result is the basis of the classical theory of straight crack motion. The calculation of the static stress intensity factor is a much easier task than the evaluation of its dynamical counterpart, since it requires solutions of bi-Laplace equations with boundary conditions. Rewriting Eq. (2) in the light of this result one obtains

$$\Gamma(v) = \frac{1}{E}A_{\rm I}(v)[k_{\rm I}(v)K^s_{\rm I}(L)]^2. \tag{4}$$

A further serendipitous simplification arises from numerical evaluations of the combination $A_{\rm I}(v)k^2_{\rm I}(v)$, showing that it is well approximated by [9]

$$A_{\rm I}(v)k^2_{\rm I}(v) \approx 1 - v/c_R. \tag{5}$$

This approximation leads to an ordinary differential equation for the crack length. If one asserts that the fracture energy Γ is v independent this differential equation becomes explicit,

$$\frac{dL(t)}{dt} \approx c_R\left[1 - \frac{E\Gamma}{[K^s_{\rm I}(L(t))]^2}\right]. \tag{6}$$

It should be stressed again that the decomposition property of the dynamic stress intensity factor [Eq. (3)] is essential in deriving this basic equation. This equation predicts a monotonic increase in the tip velocity asymptoting towards c_R. There is no crack motion as long as the stress intensity factor does not exceed a material dependent threshold

$$K^s_{\rm I}(L(t)) < \sqrt{E\Gamma} \text{ no crack motion}. \tag{7}$$

For the sake of illustration we show in Fig. 2 the solution of this equation for the simple case $K^s_{\rm I}(L(t)) = \sigma^\infty\sqrt{\pi L(t)/2}$, where σ^∞ is the load at infinity.

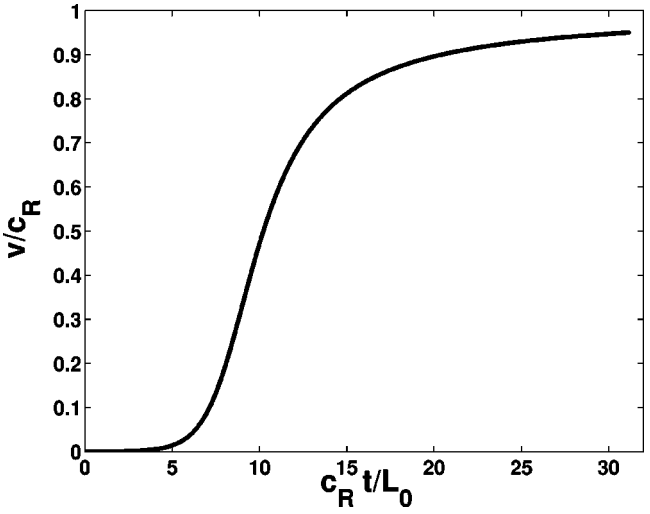

FIG. 2. The predicted velocity increase as a function of normalized time (where L_0 is the crack length at initiation) for a mode I crack under uniform constant load at infinity, Eq. (6).

B. Motivation II: bifurcating cracks

The bifurcation of fast cracks is observed in many experiments, and understanding it theoretically is a problem of some importance in the theory of fracture. One interesting problem that was addressed recently [12] in this context is

the determination of the stress intensity factors at the tips of symmetrically branched cracks in terms of the stress intensity factor prior to branching. Reference [12] presented a solution to this problem for mode III (antiplane) conditions. In this solution the stress intensity factor K' at the tips of two symmetric branches emerging from a macrocrack at a velocity v' and creating an angle $\lambda\pi$ relative to the macrocrack line, was given in the form

$$K' = \sqrt{1 - v'/c_s}\, H_{33}(\lambda, v'/c_s) K_0. \tag{8}$$

Here $\sqrt{1-v'/c_s}$ is the mode III universal function, whose mode I counterpart is $k_{\mathrm{I}}(v)$, c_s is the shear wave speed, K_0 is the stress intensity factor of the macrocrack prior to branching and $H_{33}(\lambda, v'/c_s)$ carries the information regarding the dynamic interaction. Note that the macrocrack velocity v is absent here as in the branching scenario adopted in Ref. [12] the macrocrack stops suddenly before branching and a static stress distribution is established behind a wave front traveling at the characteristic wave speed c_s. If the decomposition in Eq. (3) is of some generality then we expect the main interaction effect to be contained in the *static* stress intensity factors for the bifurcated configuration given by $H_{33}(\lambda, 0)K_0$. Indeed, Fig. 4 in Ref. [12] shows that the ratio

$$\frac{H_{33}(\lambda, v'/c_s)}{H_{33}(\lambda, 0)} \tag{9}$$

is very close to unity (up to ±5%) for all the values of λ and v'/c_s. Therefore, we conclude that even for this complex configuration the dynamic stress intensity factor admits an approximate decomposition in the form of a product of its static counterpart and a universal function of the local crack tip velocity,

$$K' \approx \sqrt{1 - v'/c_s}\, H_{33}(\lambda, 0) K_0. \tag{10}$$

This result suggests that a very good approximation for the *dynamic* stress intensity factor can be obtained by calculating the *static* stress intensity factor for the same instantaneous configuration and a knowledge of a universal velocity function characteristic of the local symmetry conditions at the crack tip.

C. The decomposition approximation for our problem

For advancing the problem posed in this paper we need to consider the stress field in the vicinity of three crack tips. In the vicinity of the tip of the macrocrack we write [in the local polar coordinates $(r_{\mathrm{M}}, \theta_{\mathrm{M}})$ around that tip]

$$\sigma_{ij}(r_{\mathrm{M}}, \theta_{\mathrm{M}}, t) = K_{\mathrm{M}} \frac{\Sigma_{ij}^{\mathrm{I}}(\theta_{\mathrm{M}}, v_{\mathrm{M}}(t))}{\sqrt{2\pi r}}, \tag{11}$$

where K_{M} is the stress intensity factor that in principle depends on the positions and velocities of all the tips [i.e., $L(t), \ell_{\pm}(t), v_{\mathrm{M}}(t), v_{\pm}(t)$] and maybe other derivatives. Near the tips of the microcrack we write similarly [in local polar coordinates $(r_{\pm}, \theta_{\pm})$ around each tip]

$$\sigma_{ij}(r_{\pm}, \theta_{\pm}, t) = K_{\pm} \frac{\Sigma_{ij}^{\mathrm{I}}(\theta_{\pm}, v_{\pm}(t))}{\sqrt{2\pi r}}, \tag{12}$$

where $K_{\pm}$ are again the stress intensity factors that depend on all the time dependent functions $L(t), \ell_{\pm}(t), v_{\mathrm{M}}(t), v_{\pm}(t)$ and maybe other derivatives.

Our basic approximation is now motivated by the two examples, Eqs. (3) and (10); we assume that the dynamic stress intensity factors can be decomposed according to

$$\begin{aligned} K_{\mathrm{M}} &\approx k_{\mathrm{I}}(v_{\mathrm{M}}) K_{\mathrm{M}}^{s}(L(t), \ell_{+}(t), \ell_{-}(t)), \\ K_{+} &\approx k_{\mathrm{I}}(v_{+}) K_{+}^{s}(L(t), \ell_{+}(t), \ell_{-}(t)), \\ K_{-} &\approx k_{\mathrm{I}}(v_{-}) K_{+}^{s}(L(t), \ell_{+}(t), \ell_{-}(t)). \end{aligned} \tag{13}$$

Here the universal function $k_{\mathrm{I}}(v)$ is the *same* function appearing in Eq. (3) and all the stress intensity factors with superscript *s* refer to the solution of the *static* problem with a frozen geometry which is given by the crack tip positions $L(t), \ell_{\pm}(t)$. On physical grounds we expect this approximation to be good when $\ell/L \to 0$, and to lose its validity as this ratio increases. The numerical simulations presented in Sec. V lend a strong support to this expectation.

The advantage of this approximation is that it leads to ordinary differential equations for the tip positions in much the same way that Eq. (6) followed from Eq. (3),

$$\begin{aligned} \frac{dL(t)}{dt} &\approx c_R \left[1 - \frac{E\Gamma}{[K_{\mathrm{M}}^{s}(L(t), \ell_{+}(t), \ell_{-}(t))]^2} \right], \\ \frac{d\ell_{-}(t)}{dt} &\approx c_R \left[1 - \frac{E\Gamma}{[K_{-}^{s}(L(t), \ell_{+}(t), \ell_{-}(t))]^2} \right], \\ \frac{d\ell_{+}(t)}{dt} &\approx c_R \left[1 - \frac{E\Gamma}{[K_{+}^{s}(L(t), \ell_{+}(t), \ell_{-}(t))]^2} \right]. \end{aligned} \tag{14}$$

We turn now to the analysis of this set of equations and their consequences.

IV. SOLUTION OF THE MODEL

A. The static problem

A prerequisite to the solution of the set of equations (14) is the calculation of the static stress intensity factors for a general configuration of two collinear cracks. We employ the available solution for two collinear cracks consisting of segments $a<x<b$ and $c<x<d$ with $b<c$ under a remote mode I loading σ^{∞}. The σ_{yy} component of the stress tensor along the cracks line, outside the cracks, is given by [13]

$$\sigma_{yy}(x,0) = \frac{\sigma^{\infty}}{2G(x)} \left(2x^2 - (a+b+c+d)x + ab + cd - (d-b) \times (c-a) \frac{\mathbf{E}(m)}{\mathbf{K}(m)} \right). \tag{15}$$

Here

$$G(x) = \sqrt{(x-a)(x-b)(x-c)(x-d)},$$

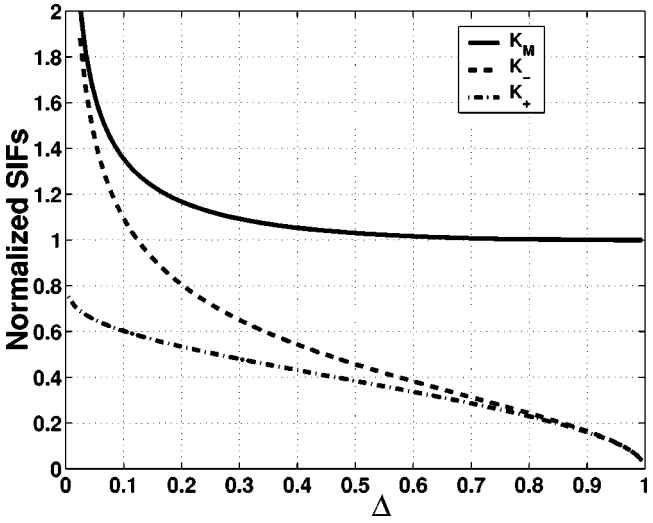

FIG. 3. The normalized static stress intensity factors (SIFs) as a function of Δ. The normalization factor is $\sigma^{\infty}\sqrt{\pi L/2}$, which is the stress intensity factor of the macrocrack in the absence of the microcrack. We fixed $\ell_+=1$ and varied ℓ_-. Note that the stress intensity factors obey $K_+<K_-<K_{\mathrm{M}}$ and that $K_{\mathrm{M}}\to\sigma^{\infty}\sqrt{\pi L/2}$ as the ratio ℓ/Δ decreases, as expected.

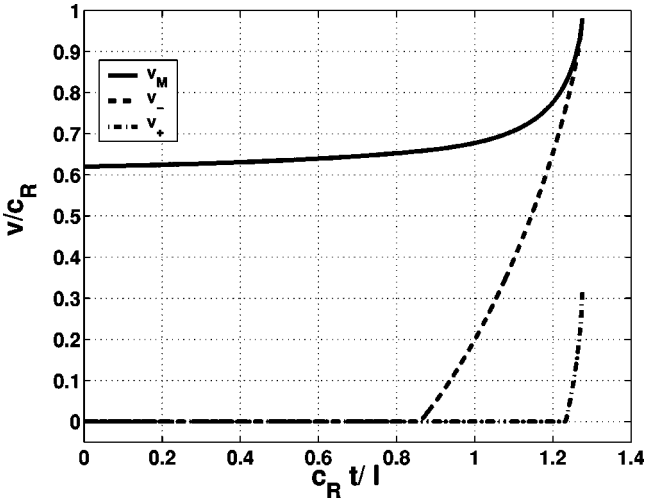

FIG. 4. The three crack tip velocities for an interaction event when a macrocrack traveling at an initial velocity $v_{\mathrm{M}}=0.62c_R$ interacts with a collinear microcrack of length $\ell=5$ positioned at $\Delta=5$. The figure shows the normalized velocities v/c_R as a function of the normalized time c_Rt/ℓ.

$$m=\frac{(d-c)(b-a)}{(d-b)(c-a)}, \tag{16}$$

and **E** and **K** are the complete elliptic integrals of the first and second kind [14]. The stress intensity factor at any one of the tips is obtained by taking the limit

$$K_i=\lim_{x\to x_i}\sqrt{2\pi(x-x_i)}\sigma_{yy}(x,0), \tag{17}$$

where x_i is any one of positions of the tips.

In order to adapt the general configuration to our macrocrack and microcrack configuration we set $a=-L$, $b=0$, $c=\ell_-$, $d=\ell_+$. Taking the limits in Eq. (17), under the assumption $L\gg\ell$, we can extract the stress intensity factors at the three tips [15]

$$\frac{K_{\mathrm{M}}}{K^N}\approx\sqrt{\frac{\ell_+}{\ell_-}}\frac{\mathbf{E}(1-\ell_-/\ell_+)}{\mathbf{K}(1-\ell_-/\ell_+)},$$

$$\frac{K_-}{K^N}\approx\left[\left(\frac{\ell_+}{\ell_-}\frac{\mathbf{E}(1-\ell_-/\ell_+)}{\mathbf{K}(1-\ell_-/\ell_+)}-1\right)\frac{1}{\sqrt{\ell_+/\ell_--1}}\right],$$

$$\frac{K_+}{K^N}\approx\left[\left(1-\frac{\mathbf{E}(1-\ell_-/\ell_+)}{\mathbf{K}(1-\ell_-/\ell_+)}\right)\frac{1}{\sqrt{1-\ell_-/\ell_+}}\right]. \tag{18}$$

Here $K^N\equiv\sigma^{\infty}\sqrt{\pi L/2}$ is the nominal stress intensity factor of the macrocrack in the absence of the microcrack and serves here as the scale of the three stress intensity factors. In Fig. 3 we present the three stress intensity factors as a function of Δ. In this example we kept the macrotip at L and the right microtip at ℓ_+ fixed while ℓ was changed. We note that the stress intensity factor of the macrocrack goes to the single crack result (unity in the reduced coordinates of Fig. 3) when $\ell/\Delta\to 0$. Similarly, the stress intensity factor at ℓ_+ goes to unity when $\Delta\to 0$, since also in that limit we remain with one crack. This last fact is not easily seen in Fig. 3 since the upturn towards unity is very rapid, occurring just before coalescence.

B. The dynamic problem

Using the static stress intensity factors Eqs. (18) in Eqs. (14) we can solve numerically for the dynamics of the three tip positions. An example of the ensuing dynamics is exhibited in Fig. 4. We note that what is seen in this picture is typical to all the conditions that we have considered: the macrocrack is first accelerated, then the left tip of the microcrack meets the fracture criterion Eq. (7) and accelerates towards the macrocrack; after some time lag, the right tip meets the fracture criterion and starts to move and attains at coalescence a lower velocity than the original macrocrack.

To connect to velocity fluctuations observed in experiment we reinterpret the data in Fig. 4 as they would be seen by an observer. We are physically motivated by the fact that as a result of a finite measurement resolution, below a critical separation Δ_c the macrocrack tip and the outer tip of the microcrack are indistinguishable and the measured velocity is a result of some averaging. For the sake of illustration, we define the experimental velocity v_{expt} as

$$v_{\mathrm{expt}}\equiv\begin{cases}v_{\mathrm{M}} & \text{for } \Delta>\Delta_c,\\ (v_{\mathrm{M}}+v_+)/2 & \text{for } \Delta<\Delta_c.\end{cases} \tag{19}$$

Figure 5 shows the experimental velocity v_{expt} during an interaction event. The rise in velocity after the steep decline is the second of Eqs. (19). The last branch in which the velocity returns to the precollision value is out of the scope of the present model and had been added by hand for the sake of illustration. The point to stress is that the dynamic interaction event generates a typical large and rapid velocity "fluctuation" and that any other reasonable definition of v_{expt}

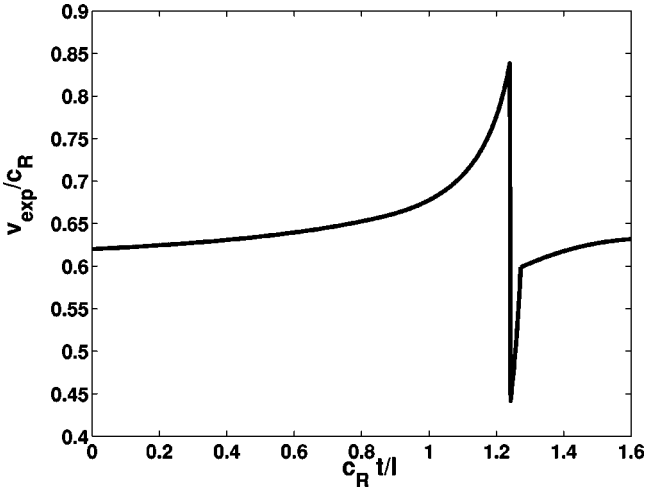

FIG. 5. The normalized experimental velocity v_{expt}/c_R as a function of the normalized time $c_R t/\ell$. The experimental velocity was calculated according to Eq. (19) with $\Delta_c \ll \ell$.

will have a qualitatively similar outcome. It should be noted that we do not consider here the effect of the nucleation of the microcrack on the macrocrack velocity. Physically we expect this effect to produce a sudden deceleration of the macrocrack prior to the effect shown in Fig. 5; this is expected since the energy supply to the crack tip region should be partitioned between the nucleation process of the microcrack and the fracture process of the macrocrack. This effect will be taken into account in future work where our current model will be coupled to a reasonable nucleation theory.

V. SIMULATIONAL SUPPORT

Since our reduction to ordinary differential equations rests on the *assumption* of the product structure (13) for the dynamic stress intensity factors, we must test the quality of the approximation by numerical simulations. We employ lattice simulations as described below.

A. Lattice simulations

Lattice models [16–22] provide a convenient, concrete, and physically sensible method of realizing crack dynamics. The material is represented by a lattice of mass points connected by Hookean springs. Fracture is achieved when a spring exceeds a certain critical extension. In certain special cases, analytic solutions for static and steadily moving cracks can be obtained. In general, the model can be easily simulated. A major advantage of this class of models is that the process zone is quite small, on the order of a few lattice spacings. Thus, already on scales of 50 or so lattice spacings, continuum dynamics is very well realized. It has been recently demonstrated [23] that the universality assumption underlying linear elastic fracture mechanics, namely, that the instantaneous crack velocity is only a function of the stress intensity factor at that moment, is extremely well satisfied by the lattice dynamics.

For our present purposes, we use the machinery developed in Ref. [23]. We solve the equilibrium elastic problem by replacing the continuum by a square lattice of mass points interacting via Born springs. The symmetry about the midline allows us to use a half-lattice with boundary conditions $u_x(x,-y)=u_x(x,y)$, $u_y(x,-y)=-u_y(x,y)$. There are springs connecting both nearest-neighbor and next-nearest-neighbor points, with the relative spring constants adjusted to give isotropic elasticity at quadratic order.

The most difficult part of the computation is the equilibration of the initial crack. The crack propagation itself happens at relatively high speed (a finite fraction of the speed of sound). However, the equilibration proceeds at a rate controlled by the longest wave lengths in the problem. Since the operator that stems from linear elasticity is fourth-order in spatial derivatives, the time to relax the lattice scales as W^4, in real time units. Since the computational cost of a single update of the entire lattice scales as W^2, it is clear that a simple relaxation algorithm is prohibitive. However, the lack of an intrinsic scale in linear elasticity comes to the rescue, as the problem is ideally suited for a multigrid approach [24,25]. The main idea is that we are trying to solve what is, at the longest and most troublesome scales, a continuum elasticity problem. We are free to solve this problem using any latticization we choose. We can obtain good information on the large-scale structure of the solution very cheaply using a very coarse lattice, and use a fine lattice to obtain the short-scale information we are still missing.

In practice, we begin with the formulation of the problem on the original fine lattice. Instead of solving this problem directly, we coarsen the grid by a fixed factor. The crack length, of course, also shrinks by the same factor (in practice, we choose the scale factor to keep the crack length as close as possible to an integer number of lattice units). This formulates a new problem. We solve this new problem in the same way, by reformulating it on a yet coarser lattice. The coarsest lattice we choose is one in which the crack is a few lattice sites long, since any further coarsening would remove the crack altogether. This coarsest problem is solved by relaxation. The solution is then lifted to the next finer lattice via bicubic spline interpolation [25]. This actually amounts to extrapolation for the lattice points in the fine lattice which are not contained in the coarse half-lattice. The interpolation introduces some amount of high spatial frequency noise, which we eliminate by performing a moderate number of relaxation sweeps. We thus proceed up the chain until we have a solution on the original fine scale. This solution is much better than the original, typically the largest residual (unbalanced force on a mass) has been reduced by 2–3 orders of magnitude.

We now refine the solution by writing $u_{x,y}=u^0_{x,y}+u^1_{x,y}$, where u_0 is the solution we have found to date. The residual field satisfies an inhomogeneous equation, where the inhomogeneity is the residual resultant forces on each lattice mass. We then invoke our whole multigrid apparatus on this new inhomogeneous problem. This procedure reduces the residual by typically another order of magnitude. Another few rounds of this game give us solutions with residuals of order 10^{-9} or less. As we are interested in cracks that propagate along the midline, we allow only bonds that cross the midline to break. We start with a square lattice with $W=801$ under fixed-displacement loading at the top and bot-

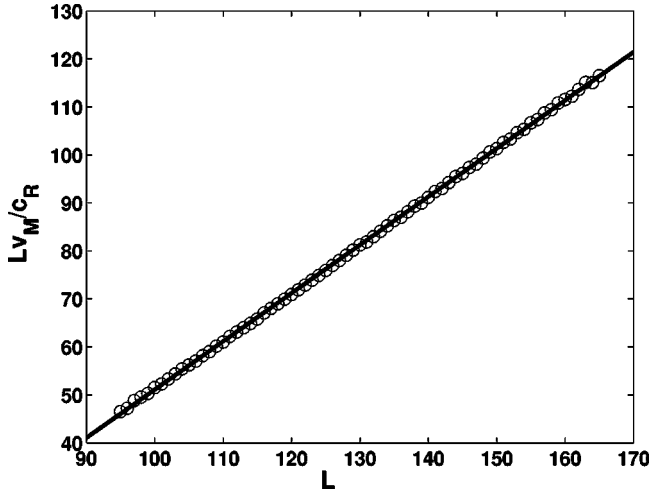

FIG. 6. The simulation data of Lv_M/c_R as a function of L are shown by the circles and the linear fit for these data is shown by the solid line. It is clear that the functional form suggested by Eq. (20) indeed describes the single crack dynamics in the lattice simulation. The fit is consistent with the assumptions since the slope α is very close to 1.

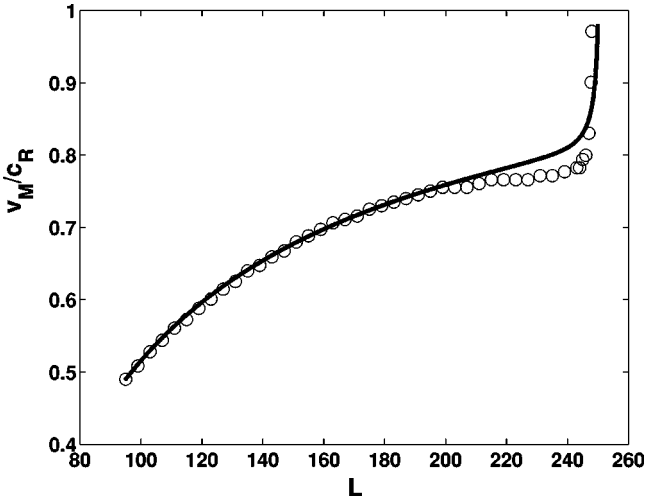

FIG. 7. The simulation data of v_M/c_R as a function of L are shown by the circles and the analytic approximation predictions are shown by the solid line. In this simulation we used $L \approx 245$ (the length of the macrocrack in the interaction region) and $\ell = 10$. The analytic approximation predicted the simulated data up to an error of 6.5%, even though the ratio L/ℓ was not very large.

tom, with bonds broken according to the desired initial configuration, Fig. 1. At this point, we manually break the bond at the end of the macrocrack, and monitor the subsequent sequence of bond breakings.

B. Results of lattice simulations

In order to test the quality of the product structure approximation we should first show that the analytic equation (6) for the dynamics of a *single* macrocrack describes correctly the corresponding dynamics in the lattice simulations. Multiplying Eq. (6) by L we obtain

$$L\frac{v_M}{c_R} = \alpha L + \beta, \tag{20}$$

where α is predicted to equal 1. The parameter β relates the material properties and boundary conditions of the lattice experiment to those in the continuum model. We simulated a single crack propagating without any additional damage, and measured v_M/c_R as a function of L. Next we fitted the data to Eq. (20). Figure 6 shows that the functional form given by Eq. (20) describes well the single crack dynamics in the lattice simulation. Moreover, we found that $\alpha \approx 1$; thus our procedure appears internally consistent. It should be noted that, notwithstanding the excellent agreement evidenced in Fig. 6, there are a number of uncontrolled approximations at play here. First, the functional form in Eq. (20) is based on the assumption of a constant fracture energy. In fact, the fracture energy for our theoretical "lattice" material has been calculated, and it is not constant. Second, the simulation employs constant displacement boundary conditions in a finite strip (though, in order to mimic infinite medium, we specialized for times that do not allow wave interactions with the outer boundaries), and the theory assumes fixed stress at infinity. The excellence of the fit despite all this is somewhat unexpected, and bears further study.

To directly test our product structure approximation, Eqs. (13), we used the value of β obtained by the linear fit and performed lattice simulation where a macrocrack interacts with a collinear microcrack. We encounter a difficulty in the simulations since the microcrack tips were trapped even when the stress intensity factor exceeds the material threshold (7). This known phenomenon of lattice trapping is an artifact of the lattice structure; to overcome it we fixed the microcrack tips also in the analytic calculation. An example of the comparison between the simulation data and the analytic approximation is shown in Fig. 7. We found that our analytic approximation agrees with the simulated data, with deviations that are typically small. The largest errors are smaller than about 6%–7% even for $L/\ell \approx 25$. For larger ratios, which is the expected physical regime, we expect better approximations. Note that the fact that the analytic approximation overestimates the velocity of the macrocrack is expected on physical grounds. Our product structure approximation relies on the fact that for short distances the information on the positions of the crack tips, carried by elastic waves, flows almost instantly even if the typical crack propagation velocities are of the order of c_R. In reality it takes finite time for the stresses to reorganize themselves according to the new crack tip positions and generally the energy release rate is lower than in our approximation.

The main conclusion of this section is that the product structure approximation, Eqs. (13), gives very good predictions for the model problem studied here. We propose to interpret this in a broader way, and to test the applicability of this approximation in other contexts.

VI. SUMMARY AND CONCLUSIONS

This study has two aims; on the one hand, we are interested in the velocity fluctuations seen in dynamical crack

propagation, and proposed here that the linear-elastodynamics interactions with microcracks may very well be responsible for them. We did not address the reasons for the existence of the microcracks—these may be there *ab initio* or get born by the high stresses near the tip of the advancing cracks. On the other hand, we are after simplified methods of analysis of crack propagation in nontrivial environments. The technical difficulty of solving the full dynamical equations calls for approximate methods that work. With the motivation presented in Sec. III we demonstrated how the assumption of the product structure for the stress intensity factors reduces the dynamics to a set of ordinary differential equations that are easily solved. The gratifying agreement with the lattice simulations emboldens us to propose this as an approach that may find applications in other contexts of interest. Only future work will help to strengthen or delineate the usefulness of this approach.

To further connect the interaction model to experimental observations one should couple our theory to a physically motivated model that will determine the conditions for microcracks nucleation. Such a model will potentially predict the appearance of distributed damage in the process zone and the interaction with the macrocrack may be related to the roughness of crack surfaces and the periodicity of the velocity fluctuations.

ACKNOWLEDGMENTS

This work had been supported in part by the European Commission through a TMR grant and by the Israel Science Foundation founded by the Israel Academy of Sciences and Humanities.

[1] K. Ravi-Chandar and W. G. Knauss, Int. J. Fract. **26**, 65 (1984).
[2] K. Ravi-Chandar and W. G. Knauss, Int. J. Fract. **26**, 141 (1984).
[3] E. Sharon, S. P. Gross, and J. Fineberg, Phys. Rev. Lett. **74**, 5096 (1995).
[4] E. Sharon and J. Fineberg, Phys. Rev. B **54**, 7128 (1996).
[5] K. Ravi-Chandar and B. Yang, J. Mech. Phys. Solids **45**, 535 (1997).
[6] K. Ravi-Chandar, Int. J. Fract. **90**, 83 (1998).
[7] E. Sharon and J. Fineberg, Nature (London) **333**, 397 (1999).
[8] J. Fineberg and M. Marder, Phys. Rep. **313**, 1 (1999).
[9] L. B. Freund, *Dynamic Fracture Mechanics* (Cambridge University Press, Cambridge, 1998).
[10] L. B. Freund, J. Mech. Phys. Solids **20**, 141 (1972).
[11] B. V. Kostrov, Int. J. Fract. **11**, 47 (1975).
[12] M. Adda-Bedia J. Mech. Phys. Solids **52**, 1407 (2004).
[13] K. B. Broberg, *Cracks and Fracture* (Academic, New York, 1999).
[14] M. Abramowitz and I. A. Stegun, *Handbook of Mathematical Functions* (Dover, New York, 1975).
[15] L. R. F. Rose, J. Am. Ceram. Soc. **69**, 212 (1986).
[16] L. I. Slepyan, Sov. Phys. Dokl. **26**, 538 (1981).
[17] Sh. A. Kulamekhmetova, V. A. Saraikin, and L. I. Slepyan, Mech. Solids **19**, 102 (1984).
[18] M. Marder and X. Liu, Phys. Rev. Lett. **71**, 2417 (1993).
[19] M. Marder and S. Gross, J. Mech. Phys. Solids **43**, 1 (1995).
[20] D. A. Kessler and H. Levine, Phys. Rev. E **59**, 5154 (1998).
[21] D. A. Kessler, Phys. Rev. E **61**, 2348 (2000).
[22] L. Pechenik, H. Levine, and D. A. Kessler, J. Mech. Phys. Solids **50**, 583 (2002).
[23] D. A. Kessler and H. Levine, Phys. Rev. E **68**, 036118 (2003).
[24] A. Brandt, Math. Comput. **31**, 333 (1977).
[25] W. H. Press, S. A. Teukolsky, W. T. Vetterling, and B. P. Flannery, *Numerical Recipes in Fortran 77: The Art of Scientific Computing*, 2nd ed. (Cambridge University Press, Cambridge, 1992).